High-Precision Extraction of Tree Parameters and Forest Structure Analysis Using Airborne LiDAR in Western Romania

Ioana VIZIREANU, Georgiana GRIGORAȘ, Dan RĂDUCANU, Lucian Marius NECULA, and Liviu PORUMB

***Abstract*—This study evaluates two airborne LiDAR workflows for individual-tree delineation in a temperate mixed forest near Runcu Mare, Hunedoara County, Romania. A 3D point-cloud segmentation is compared with a CHM-based raster approach using marker-controlled watershed segmentation. From both outputs, key metrics—tree height, crown diameter, crown area and crown volume—were derived. Quantitative comparison on a representative patch shows that the point-cloud method detects ~12% more trees (3620 vs 3240) and yields ~27% smaller mean crown areas (23.2 vs 31.8 m²) than the raster workflow, while height estimates are similar. Spatial statistics on a 1 km² subset indicate a unimodal nearest-neighbour distance (mean 3.9 ± 1.2 m) and significant clustering at d < 10 m from Ripley's K(d). At landscape scale (~22 km²), the point-cloud method identified 21684 trees and enabled mapping of density and structural contrasts across stands. Overall, the 3D approach provides higher spatial precision and more realistic crown geometry, whereas the CHM method remains efficient for rapid, broad-area mapping. The workflow supports applications in forest inventory, carbon accounting, and ecological monitoring.**

***Index Terms*—Airborne LiDAR, individual-tree delineation, point-cloud segmentation, canopy height model, nearest-neighbour distance, Ripley's K, forest structure.**

I. Introduction

Forests are complex socio-ecological systems that regulate climate, conserve biodiversity, and sustain essential ecosystem services ranging from carbon storage to water security and livelihoods [1]. Credible, policy-relevant monitoring hinges on structural information at the individual-tree level—height, crown geometry, and volume—because these variables underpin biomass estimation, condition assessment, and the design of sustainable management interventions. In this context, airborne LiDAR has become a reference technology for resolving three-dimensional forest structure with high spatial fidelity, including in mountainous terrain where conventional inventories are constrained by access and visibility.

Over the past decade, LiDAR methodologies have progressed from canopy-surface descriptions to individual-tree delineation based on both raster and point-cloud workflows [2]. In mixed-species settings, approaches that rely on canopy height models (CHMs) often provide robust height estimates compared with methods that use only normalised point clouds, owing to smoother signal-to-noise characteristics at the canopy surface [3]. Building on these representations, segmentation techniques such as marker-controlled watershed, density-based clustering, and graph-based models have demonstrated strong performance in separating adjacent crowns under dense canopies and complex stand structures [4]. Complementary developments in direct 3D clustering leverage the vertical profile of the point cloud to distinguish neighbouring trees and to better retain crown geometry in heterogeneous forests [5].

Concurrently, the emergence of sensor-agnostic deep-learning frameworks has broadened scalability and generalisability across forest types and acquisition conditions [6]. The availability of curated, open benchmark datasets enables transparent comparisons of algorithms, training regimes, and post-processing rules, thereby strengthening reproducibility and transferability across sites [7, 8]. At the level of ecological inference, LiDAR-derived individual-tree attributes—particularly height, crown diameter/area, and crown volume—have been shown to enhance models of above-ground biomass and related functional indicators across diverse environments [9, 10].

This scientific momentum aligns with climate and biodiversity policy frameworks that call for rigorous, spatially explicit tracking of forest condition. Initiatives such as REDD+ and the EU Forest Strategy for 2030 promote advanced Earth-observation tools to monitor degradation, recovery, and management outcomes, with LiDAR increasingly recognised as a benchmark data source for inventories and carbon accounting [11, 12]. Despite this progress, tree-level segmentation and multivariate structural analysis remain comparatively under-represented in Central and Eastern Europe, where many studies have focused on terrain modelling or broad-scale biomass mapping rather than crown-level delineation [13, 14].

Addressing this gap requires replicable workflows that can be applied in topographically complex, species-rich

I. VIZIREANU is with the Military Technical Academy "Ferdinand I", and the INCAS - National Institute for Aerospace Research "Elie Carafoli", Bucharest, Romania (email: vizireanu.ioana@incas.ro).

G. GRIGORAȘ is with the INCAS - National Institute for Aerospace Research "Elie Carafoli", Bucharest, Romania (email: grigoras.georgiana@incas.ro).

D. RĂDUCANU is with the Military Technical Academy "Ferdinand I", Bucharest, Romania (email: dan.raducanu@gmail.com).

L.M. NECULA is with the Military Technical Academy "Ferdinand I", Bucharest, Romania (email: marius.lucian.necula@gmail.com).

L. PORUMB is with the Military Technical Academy "Ferdinand I", Bucharest, Romania (email: porumb_liviu@yahoo.com).

Digital Object Identifier 10.32754/JMT.2026.1.20

temperate forests and that yield metrics suitable for both ecological analysis and decision-support. The present study contributes in this direction by evaluating two complementary segmentation strategies in a temperate mixed forest of the Southern Carpathians: a raster-based CHM workflow that detects local maxima and segments crowns via marker-controlled watershed, and a direct 3D point-cloud workflow that clusters vegetation returns in space. From these delineations, a consistent set of individual-tree metrics is derived—height, crown diameter, crown area, and crown volume—and examined for agreement and bias between methods, with attention to crown-shape realism and the detection of suppressed trees in dense stands.

Beyond segmentation accuracy, an understanding of spatial organisation at tree level is essential to interpret competition, regeneration, and disturbance legacies. Accordingly, the analysis considers tree-density mapping and spatial-pattern indicators, combining nearest-neighbour distance to capture local spacing with Ripley's K to assess clustering across multiple scales [15, 16]. The resulting diagnostics provide complementary evidence on how structural attributes co-vary in space and how method choice influences the detection of dense clusters versus sparse edge conditions.

Taken together, the integrative approach—linking raster- and point-cloud-based delineations with individual-tree metrics and spatial statistics—offers a rigorous basis for tree-level forest monitoring in an under-represented European mountain context. By emphasising transparent comparison, reproducible processing, and policy-relevant indicators, the study positions airborne LiDAR as a practical instrument for ecological modelling, carbon accounting, and management planning in temperate mixed forests.

II. Study Area and Data Description

A. Study Area

The study area is located near the village of Runcu Mare in Hunedoara County, in western Romania. Positioned within the Poiana Ruscă Mountains—a subunit of the Western Carpathians (Carpații Occidentali)—the region is characterised by complex topography and predominantly deciduous forest cover [17]. The landscape features moderate to steep slopes, with elevations ranging from approximately 550 to 850 metres above sea level. The central coordinates of the area are 45.7431° N latitude and 22.6576° E longitude, based on the WGS84 reference system.

This mountainous region is sparsely inhabited and shows minimal signs of anthropogenic disturbance, providing ideal conditions for structural forest analysis. The heterogeneity of the canopy, along with variations in terrain elevation and slope orientation, makes the site particularly suitable for evaluating the performance of airborne LiDAR in individual tree segmentation and parameter extraction. The forest composition is representative of temperate broadleaf ecosystems and includes species such as beech (*Fagus sylvatica*), sessile oak (*Quercus petraea*), and hornbeam (*Carpinus betulus*) [18].

B. LiDAR Data

The LiDAR dataset used in this study was acquired during a spring airborne survey conducted by the National Institute for Aerospace Research "Elie Carafoli" (INCAS, Bucharest). The campaign used a Hawker Beechcraft King Air C90 GTx carrying a RIEGL LMS-Q680i laser scanner operating at 1,064 nm. Although the mission covered a wider area in western Romania, a smaller forested sector near the village of Runcu Mare was selected for detailed analysis.

Data acquisition took place during the leaf-off period to ensure optimal canopy penetration and accurate ground detection. Flight lines were designed in parallel, with approximately 35% side overlap between adjacent strips. The average flight altitude was 500 metres above ground level, with a cruising speed of 70 m/s. These settings yielded a nominal mean point density of ~10 points m^{-2} (all returns), adequate for individual-tree segmentation and structural analysis.

Although the full campaign spanned several hours, data acquisition over the selected study area required only a short portion of the total flight time.

III. Methodology

The main objective of this study was to evaluate and compare two LiDAR-based segmentation techniques for extracting individual tree metrics in a temperate mixed forest (broadleaf and conifer). Accurate delineation of tree crowns and the estimation of structural parameters—such as height, crown diameter, and volume—are essential for characterising forest structure and assessing ecological dynamics, particularly in complex mountainous environments.

Two complementary approaches were employed. The first was a point-cloud-based method, applied directly to the 3D LiDAR dataset. It involved classification and filtering of ground and vegetation points, followed by clustering of canopy returns based on spatial proximity and geometric characteristics. This method preserved the full three-dimensional resolution of the LiDAR data and was particularly suitable for analysing dense or overlapping canopy structures.

The second approach was a raster-based method, relying on a high-resolution Canopy Height Model (CHM) derived from airborne LiDAR data. Local maxima were detected and used as seed points for crown delineation through a marker-controlled watershed segmentation algorithm. This technique is commonly adopted due to its computational efficiency and compatibility with raster processing environments.

To ensure a fair comparison, both methods were applied to the same study area and LiDAR dataset, allowing for consistent evaluation of segmentation performance and parameter accuracy.

The complete processing workflow, from data acquisition to comparative analysis of extracted tree parameters, is summarised in Fig. 1.

 Digital Object Identifier 10.32754/JMT.2026.1.20

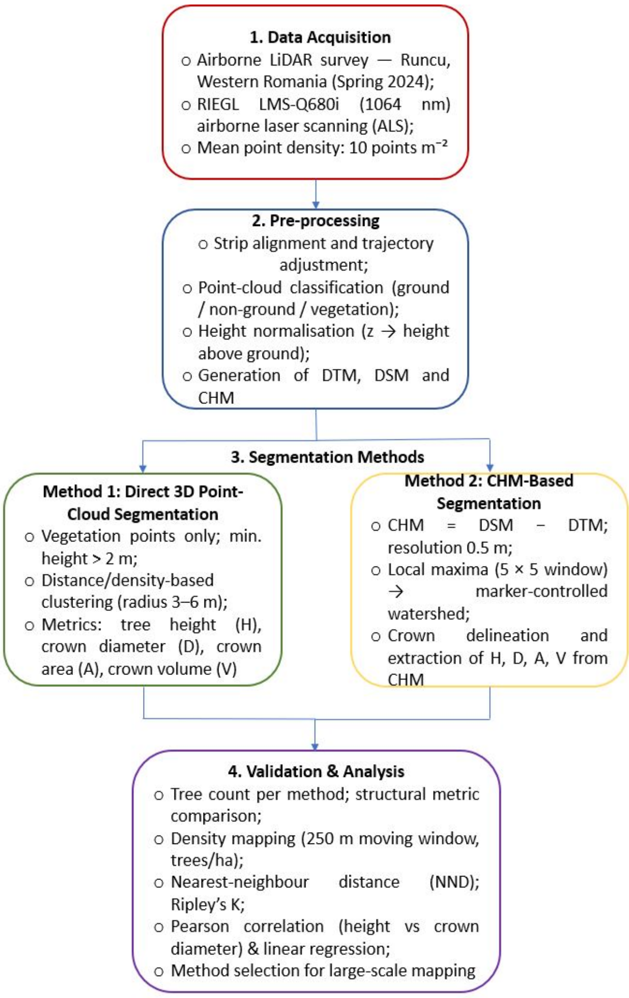

Figure 1. LiDAR-based workflow for individual tree segmentation and parameter extraction

A. Individual Tree Segmentation and Parameter Extraction

Although data preprocessing, including strip alignment, ground classification, and *CHM* generation, was carried out according to standard airborne LiDAR workflows [19, 20], the focus of this section is on the segmentation and extraction of individual tree attributes. The segmentation process followed two distinct methodological paths, both applied to the same high-resolution LiDAR dataset to ensure a consistent comparison of results.

1) 3D Point-Based Segmentation

In the first method, individual trees were segmented directly from the classified 3D point cloud. Only vegetation points were retained, after excluding ground returns based on class codes. The segmentation was performed using a clustering approach based on spatial proximity and local point density.

To separate individual trees, a distance-based clustering algorithm was applied, where each vegetation point was assigned to a tree crown based on its Euclidean distance to nearby points. A minimum height threshold of 2 m was imposed to filter out understorey vegetation and noise.

The 3D vegetation point cloud is defined as a set of points $P=\{p_1,p_2,\dots,p_n\}$, where each point p_i has coordinates (x_i,y_i,z_i). A tree crown C_k is modeled as a subset of points satisfying:

$$C_k=\{p_i\in P \mid p_i-c_k<d\} \quad (1)$$

where c_k is the centroid of cluster k, and d is a maximum allowed crown radius (typically 3–6 m, depending on local canopy structure). Clusters were refined using a density constraint to avoid over-segmentation in dense stands [21, 22].

From each cluster, tree height (H) was calculated as the maximum z value in the cluster minus the ground elevation directly below. Crown diameter (D) was defined as the maximum horizontal extent of the cluster, while crown area (A) was derived from the convex hull of the point cloud projected onto the xy plane. Finally, crown volume (V) was approximated using a parabolic crown shape (adapted from [23]):

$$V=\frac{\pi}{4}\cdot D^2\cdot H_c, \quad (2)$$

where H_c is the vertical crown extent, computed as the difference between the cluster's maximum and minimum height values. This approximation has been widely adopted in similar studies for its simplicity and practical relevance [10].

This 3D-based segmentation allows preservation of full spatial detail and is particularly suited for multilayered or overlapping canopy structures.

In addition to extracting structural metrics, a regression analysis was performed to examine the relationship between tree height (*H*) and crown diameter (*D*). A linear model was fitted using Ordinary Least Squares (OLS), a standard statistical method minimising squared residuals. Similar approaches have been validated in LiDAR-based forest allometry studies [24].

2) Raster-Based Segmentation

The second segmentation method was applied to a Canopy Height Model (*CHM*), generated by subtracting the Digital Terrain Model (*DTM*) from the Digital Surface Model (DSM). The resulting raster had a spatial resolution of 0.5 metres, which balances crown detail preservation and computational efficiency.

To detect potential tree tops, local maxima were identified using a 5 × 5 pixel moving window. This size was selected based on both visual inspection and previous studies, aiming to avoid over-segmentation in densely forested areas [25]. These local maxima served as seed points for a marker-controlled watershed segmentation, widely adopted in forestry for its ability to separate adjacent crowns based on topographic gradients in the *CHM*.

The *CHM* is described as a continuous function:

$$CHM\,(x,y)=DSM\,(x,y)-DTM\,(x,y), \quad (3)$$

where (x,y) are spatial coordinates. Each tree apex corresponds to a local maximum m_i in the *CHM*. The segmentation function $S(x,y)$ assigns each pixel to a crown region C_j, based on the minimal cost path to a nearby local maximum, subject to the topographic gradient constraint of the watershed algorithm:

$$S(x,y)=\arg\min_{m_i} D\big(m_i,(x,y)\big) \quad (4)$$

where D is a combined spatial and intensity-based distance metric.

After segmentation, individual tree metrics were computed from each crown region. Height was extracted as the CHM value at the apex. Crown diameter and area were calculated from the geometric footprint of the segment, and crown volume was approximated by integrating pixel values under the assumption of a parabolic crown shape, consistent with the model described in Section III.1.

Raster-based segmentation offers improved processing speed and integration with large-scale mapping workflows, though its accuracy is influenced by CHM resolution and surface roughness [26].

B. Accuracy Assessment and Statistical Comparison

To evaluate agreement between the two approaches, a statistical comparison was performed on height, crown diameter, and crown volume derived from both methods. Corresponding trees were matched by spatial proximity between crown centroids, using a 1.5 m threshold to account for minor positional discrepancies; only one-to-one matches were retained.

The strength of association was assessed using the Pearson correlation coefficient:

$$r = \frac{\sum_{i=1}^{n}\left(x_i-\bar{x}\right)\left(y_i-\bar{y}\right)}{\sqrt{\sum_{i=1}^{n}\left(x_i-\bar{x}\right)^2}\sqrt{\sum_{i=1}^{n}\left(y_i-\bar{y}\right)^2}} \tag{5}$$

where x_i and y_i are corresponding values of a given parameter from each method, and $\bar{x}, \bar{y}$ are their respective means [27].

In addition, scatter plots and ordinary least squares (OLS) regression were used to visualise and summarise relationships (e.g., crown diameter versus height), providing an interpretable summary of the linear association and trend. This assessment offers an objective basis for comparing accuracy and reliability and supports methodological choices in operational forest mapping and ecological monitoring [28].

C. Spatial Pattern Analysis

To assess the spatial arrangement of trees, two metrics were computed from crown centroids: nearest-neighbour distance (NND) and Ripley's K-function. NND captures local spacing variability, indicating clustering or regularity [29]. Ripley's K evaluates structure across multiple scales by comparing observed to expected point patterns; results are reported as K(d), as in Section IV.C. This analysis supports the evaluation of forest heterogeneity and segmentation performance [16].

IV. Results and Discussion

This section presents the results obtained from the segmentation and analysis of individual trees in the Runcu area, using both point-cloud and raster-based approaches. Differences between methods are illustrated and discussed based on spatial distribution, crown geometry, and derived parameters.

A. Tree Detection and Segmentation Results

Airborne LiDAR over the Runcu study area revealed clear differences between the two segmentation strategies. The raster-based approach (local maxima on the canopy height model, CHM) tended to over-merge dense crown clusters and to miss small trees adjacent to dominant canopies. In contrast, the point-cloud-based method delineated individual crowns more accurately, resolving neighbouring trees even where canopies are tightly packed.

Parameter sensitivity checks indicated that CHM smoothing and the local-maxima window strongly control raster outcomes: smaller kernels tended to over-split broad crowns, whereas larger windows promoted unwanted merging across neighbouring canopies. The point-cloud workflow, built on height-normalised 3D neighbourhoods and density-adaptive clustering, proved less sensitive to these trade-offs, maintaining consistent crown boundaries across gradients in canopy closure and scan angle.

Quality control combined overlays on CHM hillshade and intensity with simple geometry screens (compactness/elongation) to flag atypical polygons. Most residual errors concentrated along stand edges, skid trails and abrupt relief breaks—areas where canopy surfaces are either very smooth or highly discontinuous. These diagnostics support using the point-cloud delineations for downstream mapping and stand-structure metrics, while keeping a clear record of locations where manual review is advisable.

Fig. 2 presents a side-by-side comparison for a representative forest patch: (a) raster-based output and (b) point-cloud-based output. Although both methods reproduce the overall tree distribution, the point-cloud approach achieves higher spatial precision, particularly in dense areas.

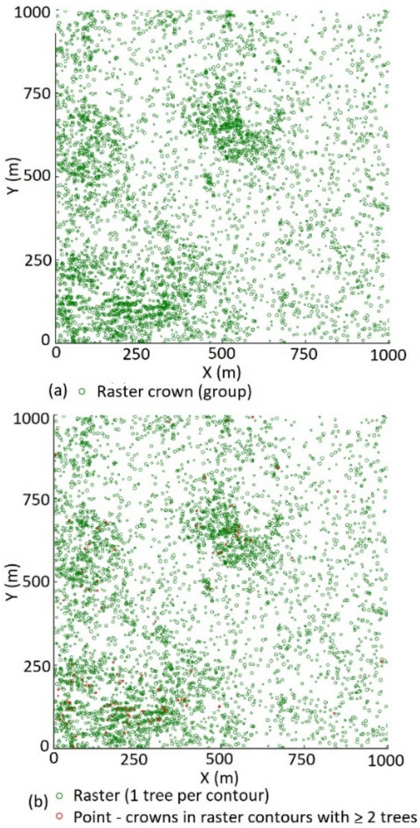

Figure 2. Tree segmentation results in a selected area of Runcu: (a) raster-based method applied to CHM; (b) point-cloud-based method

 Digital Object Identifier 10.32754/JMT.2026.1.20

To illustrate behaviour under high crown density, Fig. 3 overlays both outputs on a CHM excerpt. Green outlines depict raster-based segments, which often encompass multiple trees; red open circles mark individual crowns detected from the point cloud. Multiple red crowns occurring within a single green outline highlight raster over-merging. A 20 m scale bar provides spatial context.

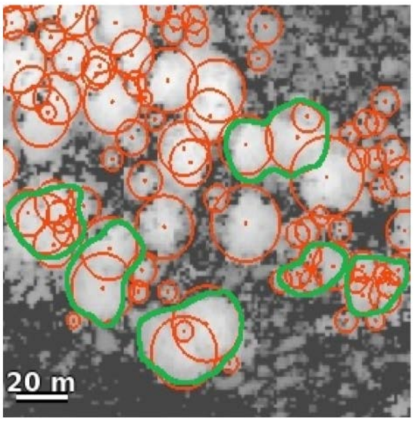

Figure 3. Raster and point-cloud–based crown delineation over a CHM excerpt

To complement the visual assessment, Table I reports a quantitative comparison. The point-cloud-based method detects more trees (3620 vs 3240; +12%) and yields smaller crowns on average (area 23.2 vs 31.8 m², −27%; diameter 4.9 vs 5.7 m, −14%), indicating finer segmentation, while mean tree height remains similar (18.1 vs 18.4 m).

TABLE I. SUMMARY STATISTICS FOR THE TWO SEGMENTATION METHODS

Parameter	Raster-Based Method	Point-Cloud-Based Method
Number of detected trees	3240	3620
Mean crown diameter (m)	5.7	4.9
Mean crown area (m²)	31.8	23.2
Mean tree height (m)	18.4	18.1

In summary, the point-cloud–based method detected ~12% more trees and yielded ~27% smaller mean crown areas than the raster approach, with comparable height estimates, and is therefore adopted for the subsequent large-scale analysis.

B. *Extrapolation to the Entire Study Area*

Based on the comparative evaluation, the point-cloud-based method was selected for large-scale tree detection across the Runcu study area. Using this approach, a total of 21684 trees were identified over approximately 22 km² of forest. At the landscape scale, tree density varies with stand type and terrain: denser clusters occur in productive mixed and conifer stands, whereas sparser patterns appear toward forest margins and along steep ridgelines.

To characterise forest structure across the full extent, crown and height attributes were summarised in Table II. The mean tree height is 14.7 m with values ranging from 3.2 to 32.5 m and a standard deviation of 5.8 m, indicating a mixture of young and mature stands. The mean crown diameter is 4.3 m (range 1.1–10.7 m, standard deviation 1.9 m). Crown area shows strong variability, with a mean of 17.4 m² (range 1.0–89.9 m², standard deviation 14.3 m²), reflecting the coexistence of small crowns in regenerating patches and larger crowns in older stands. Crown volume follows a similar pattern, with a mean of 71.2 m³ (range 4.3–412.8 m³, standard deviation 52.5 m³).

Taken together, these statistics point to marked structural heterogeneity at the landscape scale: larger and taller crowns dominate productive, mature stands, whereas smaller crowns and lower heights prevail near edges and on steep ridgelines. These metrics provide the basis for the subsequent analysis of spatial patterns and forest structure presented in the next section.

TABLE II. SUMMARY OF TREE PARAMETERS EXTRACTED ACROSS THE RUNCU STUDY AREA

Parameter	Mean	Min	Max	Standard Deviation
Tree height (m)	14.7	3.2	32.5	5.8
Crown diameter (m)	4.3	1.1	10.7	1.9
Crown area (m²)	17.4	1.0	89.9	14.3
Crown volume (m³)	71.2	4.3	412.8	52.5

C. *Spatial Analysis of Forest Structure*

The spatial distribution of trees in the Runcu area was analysed to evaluate heterogeneity, clustering tendencies, and structural complexity. Three indicators were used: tree density, nearest-neighbour distance (NND), and Ripley's K-function.

Tree density was mapped with a moving circular window of 250 m radius over a 1 km² subset of the LiDAR dataset, with values reported as trees per hectare (trees/ha). Densities were computed by counting trees within each 250 m-radius circle (area ≈ 19.6 ha), dividing by the window area, and expressing the result per hectare.

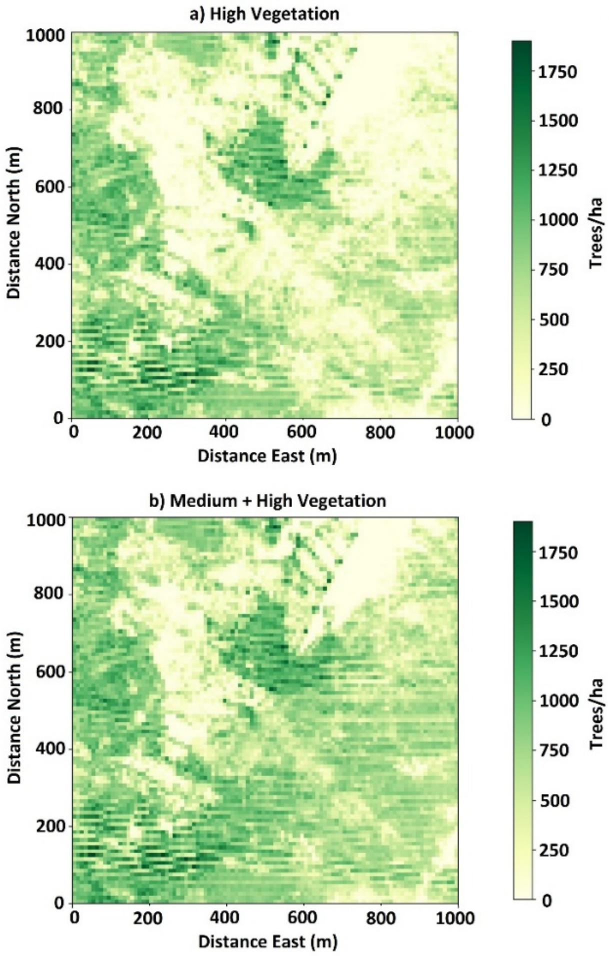

Figure 4. Tree density (trees per hectare, trees/ha) in a 1 km² subset using a 250 m-radius moving window: (a) high vegetation (> 2 m); (b) medium + high vegetation (> 0.5 m)

Fig. 4a uses only high vegetation points (>2 m), whereas Fig. 4b includes medium + high vegetation (> 0.5 m). Both maps show a heterogeneous pattern, with dense patches reaching ~1,500–1,750 trees/ha in mature or densely regenerating stands and values below ~600 trees/ha in disturbed or edge areas. Across the 1 km² subset, the mean density is 1022 trees/ha (Table III), reflecting the balance between dense cores and sparse edge/disturbed areas. Including medium vegetation increases estimated densities in early-successional zones, highlighting the effect of the height threshold on density inference.

The NND distribution (Fig. 5) is unimodal, with a mean of 3.9 m and standard deviation of 1.2 m, indicating moderate local aggregation of trees.

Clustering across spatial scales was quantified with Ripley's K-function (Fig. 6). The observed K(d) lies above the complete spatial randomness (CSR) 95% envelope for distances < 10 m, confirming significant clustering at short ranges; at larger distances the pattern approaches CSR.

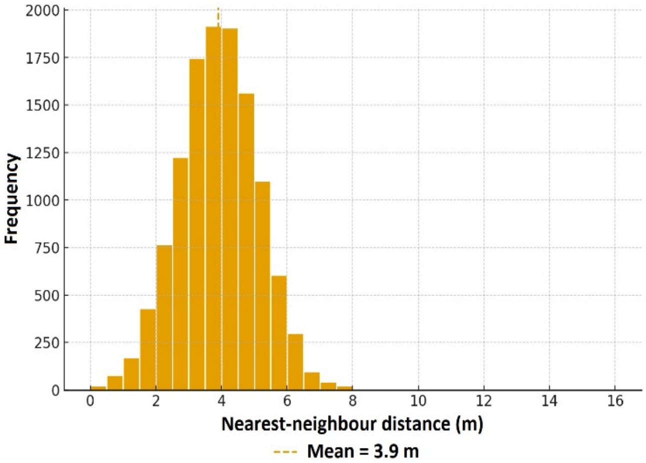

Figure 5. Histogram of nearest-neighbour distances between detected trees (mean 3.9 m, standard deviation 1.2 m)

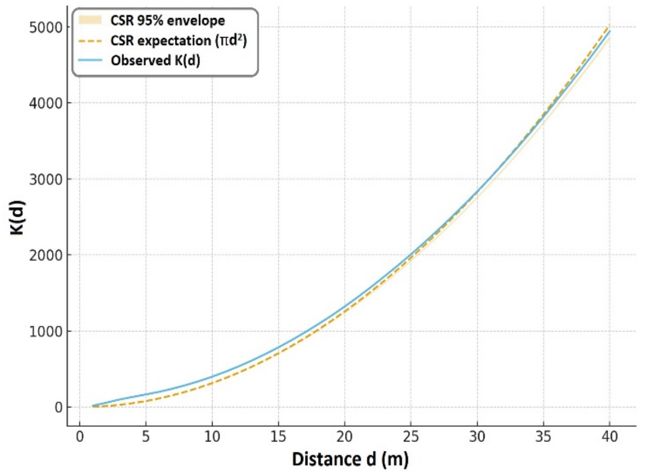

Figure 6. Ripley's K-function with the CSR 95% envelope; the observed $K(d)$ exceeds the envelope for $d < 10$ m, indicating clustering

Table III summarises the main spatial-pattern indicators derived from the analysis.

TABLE III. SUMMARY OF SPATIAL PATTERN METRICS FOR THE RUNCU FOREST AREA

Metric	Value
Tree density (subset mean, trees/ha)	1022
Nearest-neighbour distance (m)	3.9 ± 1.2
Ripley's K indication	Clustered (0–10 m)

The results confirm a non-random spatial pattern shaped by environmental gradients and forest-management history, supporting more accurate modelling of forest dynamics and providing inputs for biodiversity and fire-risk assessments.

D. Correlation Analysis and Structural Relationships

To explore the internal structure of the forest stands, a correlation analysis was conducted between key tree attributes: height, crown diameter, and crown area. These metrics were extracted using the point-based segmentation method, which demonstrated higher geometric accuracy in previous evaluations.

A Pearson correlation analysis (Fig. 7) reveals a moderately strong positive relationship between tree height and crown area ($r \approx 0.74$), indicating that taller trees generally develop larger crown areas. This relationship supports the assumption that tree dimensions are structurally interconnected.

In addition, a scatter plot in Fig. 8 illustrates the linear relationship between tree height and crown diameter. Despite some variation among age classes or species groups, the overall trend remains consistent throughout the dataset. A linear regression yielded the model:

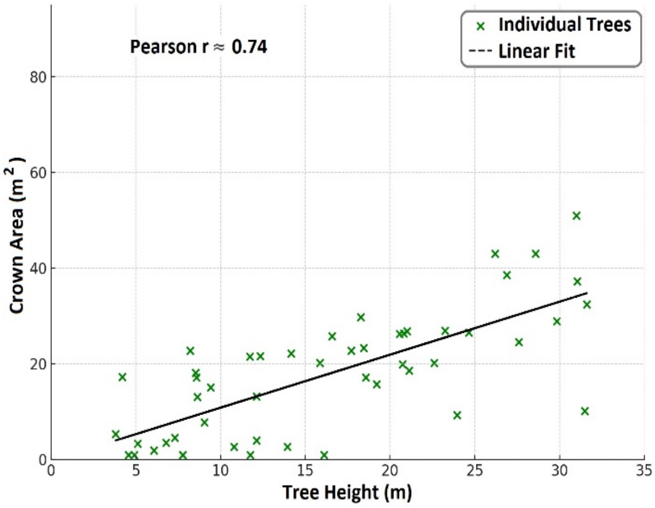

Figure 7. Pearson correlation between tree height and crown area

$$CrownDiameter = 0.35 \times TreeHeight + 0.92, \text{ with } R^2 = 0.68$$

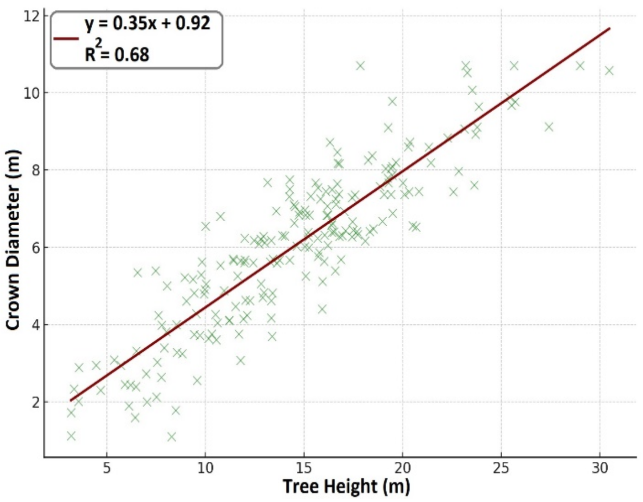

Figure 8. Scatter plot and regression line showing the relationship between tree height and crown diameter

 Digital Object Identifier 10.32754/JMT.2026.1.20

These relationships are essential for estimating forest canopy structure and serve as indicators of ecosystem dynamics in areas where direct field measurements are limited. The consistency of the patterns also reinforces the reliability of the extracted parameters.

E. Interpretation and Method Comparison

The comparison between raster- and point-based segmentation highlights clear trade-offs in accuracy, scalability, and data requirements.

The point-based approach produced the most reliable delineation of individual crowns, particularly where canopies overlap. Leveraging the 3D structure of the point cloud, it separated closely spaced trees more effectively and yielded crown shapes that better match expected geometry. These gains come at the cost of higher computational load and a dependence on sufficient point density and quality.

By contrast, the raster-based segmentation is faster and easier to embed in wall-to-wall mapping workflows, as it operates on the CHM. However, in dense stands it under-segments (merges neighbouring crowns) and misses suppressed trees near dominant stems, which tends to produce fewer but larger crowns and underestimates of tree counts.

Table IV summarises the main strengths and weaknesses observed in the Runcu case study.

TABLE IV. SUMMARY OF STRENGTHS AND WEAKNESSES FOR THE TWO SEGMENTATION METHODS

Criterion	Raster-Based Segmentation	Point-Based Segmentation
Detection of small trees / suppressed trees	Limited (often missed near dominant crowns)	Accurate when point density is adequate
Crown shape realism	Moderate (generalised outlines from CHM)	High (crowns follow 3D structure)
Behaviour in dense canopy	Under-segmentation (crown merging)	Good separation; occasional over-split in noisy data
Bias in crown metrics	Fewer, larger crowns	More trees, smaller crown areas on average
Processing time/resources	Fast, low memory	Slower, higher memory/CPU
Data requirements	CHM only	Full point cloud; sufficient point density
Integration with rasters	Seamless	Requires point-cloud processing pipeline
Suitable use cases	Rapid, regional mapping; screening	Structural analysis, biomass/individual-tree detection (ITD) monitoring

Overall, both methods are useful, but their suitability depends on objectives. For applications that require precise crown delineation and structural parameters (e.g., biomass estimation, individual-tree monitoring), the point-based method is preferable. For broad-scale mapping or rapid inventories where computational efficiency is paramount, the raster-based approach remains a practical alternative. These findings emphasise the need to match the segmentation strategy to data quality and analytical goals; in Runcu, the 3D point-based method provided higher geometric fidelity, while the raster-based method offered efficient coverage at scale.

V. LIMITATIONS AND FUTURE WORK

Despite strong overall performance, several factors bound the interpretation of our results. The method comparison was conducted without plot-level ground truth, so accuracy remains relative and supported by internal consistency and visual assessment. Both approaches are challenged by understorey/suppressed trees beneath dense overstorey, and outcomes are sensitive to analysis choices (CHM resolution, point-cloud density/quality, height thresholds, and the 250 m moving-window radius). Moreover, density maps were illustrated on a 1 km² excerpt, which may not fully capture landscape heterogeneity.

Future work will prioritise independent validation using field plots and/or high-resolution UAV/TLS data, and a targeted sensitivity analysis of key parameters to quantify uncertainty. Extending spatial statistics to inhomogeneous K, the pair-correlation g(r), and O-ring functions, and testing across additional forest types and seasons, will strengthen generalisability. Hybrid (point-cloud + CHM) or 3D learning-based delineation, embedded in a reproducible workflow, could further improve crown detection and structural metrics at scale.

VI. CONCLUSIONS

This study evaluated two individual-tree segmentation approaches from airborne LiDAR over the Runcu forest area, Western Romania: a raster-based method using CHM-derived local maxima and a point-cloud-based method operating directly in 3D. Both produced key structural metrics (height, crown diameter, crown area/volume), but with distinct performance profiles.

The point-cloud-based approach delivered higher spatial precision in dense stands, better separated closely spaced trees under overlapping canopies, and yielded crown geometries more consistent with expected shapes. It generally detected more trees with smaller crowns on average, reflecting reduced crown merging (i.e., less under-segmentation). These benefits come with greater computational cost and a dependence on point-cloud density and quality.

The raster-based approach was faster and easier to scale across large areas, but tended to miss small or suppressed trees and to merge neighbouring crowns in dense patches, thereby producing fewer but larger crowns and smoothing fine-scale structure.

Quantitative diagnostics—segmentation statistics, nearest-neighbour distances, Ripley's K, and height–crown relationships—supported the superior structural coherence of the point-cloud outputs while confirming the operational efficiency of the raster workflow. In practice, method choice should be guided by objectives: for structural analysis, biomass estimation, and individual-tree monitoring, the point-cloud-based method is preferable; for broad, rapid mapping or when resources are constrained, the raster-based method remains effective.

Overall, the results underline the value of airborne LiDAR and advanced segmentation methods for forest monitoring and inventory. When tuned to local conditions and analytical needs, these methods provide detailed structural information relevant to ecological modelling, carbon accounting, and management planning, and can be integrated into operational monitoring frameworks to support transparent, data-driven decisions.

REFERENCES

[1] FAO, *The State of the World's Forests 2022: Forest pathways for green recovery and building inclusive, resilient and sustainable economies.* Rome: FAO, 2022.

[2] Y. Pu, D. Xu, H. Wang, X. Li, and X. Xu, "A New Strategy for Individual Tree Detection and Segmentation from Leaf-on and Leaf-off UAV-LiDAR Point Clouds Based on Automatic Detection of Seed Points," *Remote Sens.*, vol. 15, no. 6, p. 1619, Mar. 2023, doi:10.3390/rs15061619.

[3] S. Chen, W. Chen, X. Sun, and Y. Dang, "Enhancing Forest Structural Parameter Extraction in the Greater Hinggan Mountains: Utilizing Airborne LiDAR and Species-Specific Tree Height–Diameter at Breast Height Models," *Forests*, vol. 16, no. 3. 2025, doi:10.3390/f16030457.

[4] J. Marcello, M. Spínola, L. Albors, F. Marqués, D. Rodríguez-Esparragón, and F. Eugenio, "Performance of Individual Tree Segmentation Algorithms in Forest Ecosystems Using UAV LiDAR Data," *Drones*, vol. 8, no. 12. 2024, doi:10.3390/drones8120772.

[5] L. Comesaña-Cebral, J. Martínez-Sánchez, H. Lorenzo, and P. Arias, "Individual Tree Segmentation Method Based on Mobile Backpack LiDAR Point Clouds," *Sensors*, vol. 21, no. 18. 2021, doi:10.3390/s21186007.

[6] M. Wielgosz, S. Puliti, B. Xiang, K. Schindler, and R. Astrup, "SegmentAnyTree: A sensor and platform agnostic deep learning model for tree segmentation using laser scanning data," *Remote Sens. Environ.*, vol. 313, p. 114367, Nov. 2024, doi:10.1016/j.rse.2024.114367.

[7] R. Puliti, S., Pearse, G., Surový, P., Wallace, L., Hollaus, M., Wielgosz, M., & Astrup, "FOR-instance: a UAV laser scanning benchmark dataset for semantic and instance segmentation of individual trees," *Zenodo*, 2023, doi:10.5281/zenodo.8287792.

[8] I. Dubrovin, C. Fortin, and A. Kedrov, "An open dataset for individual tree detection in UAV LiDAR point clouds and RGB orthophotos in dense mixed forests," *Sci. Rep.*, vol. 14, no. 1, p. 21938, 2024, doi:10.1038/s41598-024-72669-5.

[9] Y. Qiao, G. Zheng, Z. Du, X. Ma, J. Li, and L. M. Moskal, "Tree-Species Classification and Individual-Tree-Biomass Model Construction Based on Hyperspectral and LiDAR Data," *Remote Sensing*, vol. 15, no. 5. 2023, doi:10.3390/rs15051341.

[10] A. Ferraz, S. Saatchi, C. Mallet, and V. Meyer, "Lidar detection of individual tree size in tropical forests," *Remote Sens. Environ.*, vol. 183, pp. 318–333, Sep. 2016, doi:10.1016/j.rse.2016.05.028.

[11] European Comision, "Proposal for a Regulation on a monitoring framework for resilient European forests." Directorate-General for Environment, 2023, [Online]. Available: https://ec.europa.eu/transparency/documents-register/detail?ref=COM(2023)728&lang=en.

[12] R. Dubayah *et al.*, "GEDI launches a new era of biomass inference from space," *Environ. Res. Lett.*, vol. 17, no. 9, p. 95001, 2022, doi:10.1088/1748-9326/ac8694.

[13] M. A. Tanase *et al.*, "Synthetic aperture radar sensitivity to forest changes: A simulations-based study for the Romanian forests," *Sci. Total Environ.*, vol. 689, pp. 1104–1114, Nov. 2019, doi:10.1016/j.scitotenv.2019.06.494.

[14] R. Prăvălie *et al.*, "NDVI-based ecological dynamics of forest vegetation and its relationship to climate change in Romania during 1987–2018," *Ecol. Indic.*, vol. 136, p. 108629, Mar. 2022, doi:10.1016/j.ecolind.2022.108629.

[15] T. Wiegand and K. A. Moloney, *Handbook of Spatial Point-Pattern Analysis in Ecology*, Chapman and Hall/CRC, 2013.

[16] B. D. Ripley, "The second-order analysis of stationary point processes," *J. Appl. Probab.*, vol. 13, no. 2, pp. 255–266, 1976, doi: 10.2307/3212829.

[17] G. Coldea, T. Ursu, L. Filipaș, B. I. Hurdu, I.-A. Stoica, "Phytosociological research in the forests of Poiana Ruscă Mountains," *Contrib. Bot.*, vol. 50, pp. 123–135, 2015, [Online]. Available: https://contributii_botanice.reviste.ubbcluj.ro/materiale/2015/Contrib_Bot_vol_50_pp_123-135.pdf.

[18] S. Heinrichs *et al.*, "Forest vegetation in western Romania in relation to climate variables: Does community composition reflect modelled tree species distribution?," *Ann. For. Res.*, vol. 59, no. 2, Nov. 2016, doi:10.15287/afr.2016.692.

[19] J. C. White *et al.*, "A best practices guide for generating forest inventory attributes from airborne laser scanning data using an area-based approach," *For. Chron.*, vol. 89, no. 06, pp. 722–723, Dec. 2013, doi:10.5558/tfc2013-132.

[20] M. H. Wimmer, G. Mandlburger, C. Ressl, and N. Pfeifer, "Strip Adjustment of Multi-Temporal LiDAR Data—A Case Study at the Pielach River," *Remote Sens.*, vol. 16, no. 15, p. 2838, Aug. 2024, doi:10.3390/rs16152838.

[21] D. A. Coomes *et al.*, "Area-based vs tree-centric approaches to mapping forest carbon in Southeast Asian forests from airborne laser scanning data," *Remote Sens. Environ.*, vol. 194, pp. 77–88, Jun. 2017, doi:10.1016/j.rse.2017.03.017.

[22] E. Ayrey and D. J. Hayes, "The Use of Three-Dimensional Convolutional Neural Networks to Interpret LiDAR for Forest Inventory," *Remote Sens.*, vol. 10, no. 4, p. 649, Apr. 2018, doi:10.3390/rs10040649.

[23] C. A. Silva *et al.*, "Imputation of Individual Longleaf Pine (Pinus palustris Mill.) Tree Attributes from Field and LiDAR Data," *Can. J. Remote Sens.*, vol. 42, no. 5, pp. 554–573, Sep. 2016, doi:10.1080/07038992.2016.1196582.

[24] T. Jucker *et al.*, "Allometric equations for integrating remote sensing imagery into forest monitoring programmes," *Glob. Chang. Biol.*, vol. 23, no. 1, pp. 177–190, Jan. 2017, doi:10.1111/gcb.13388.

[25] K. Ma *et al.*, "Performance and Sensitivity of Individual Tree Segmentation Methods for UAV-LiDAR in Multiple Forest Types," *Remote Sens.*, vol. 14, no. 2, p. 298, Jan. 2022, doi:10.3390/rs14020298.

[26] M. Jakubowski, W. Li, Q. Guo, and M. Kelly, "Delineating Individual Trees from Lidar Data: A Comparison of Vector- and Raster-based Segmentation Approaches," *Remote Sens.*, vol. 5, no. 9, pp. 4163–4186, Aug. 2013, doi:10.3390/rs5094163.

[27] A. Nemmaoui, F. J. Aguilar, and M. A. Aguilar, "Benchmarking of Individual Tree Segmentation Methods in Mediterranean Forest Based on Point Clouds from Unmanned Aerial Vehicle Imagery and Low-Density Airborne Laser Scanning," *Remote Sens.*, vol. 16, no. 21, p. 3974, Oct. 2024, doi:10.3390/rs16213974.

[28] I. Sačkov, L. Kulla, and T. Bucha, "A Comparison of Two Tree Detection Methods for Estimation of Forest Stand and Ecological Variables from Airborne LiDAR Data in Central European Forests," *Remote Sens.*, vol. 11, no. 12, p. 1431, Jun. 2019, doi:10.3390/rs11121431.

[29] P. J. Clark and F. C. Evans, "Distance to Nearest Neighbor as a Measure of Spatial Relationships in Populations," *Ecology*, vol. 35, no. 4, pp. 445–453, Oct. 1954, doi:10.2307/1931034.

 Digital Object Identifier 10.32754/JMT.2026.1.20